

Evaluation on Failure of Fiber-Reinforced Sand

Zhiwei Gao¹ and Jidong Zhao²

Abstract: Fiber reinforcement can help to enhance soil strength, stabilize near-surface soil layers, and mitigate the risk of soil liquefaction. Evaluation of the strength of fiber-reinforced soils needs a proper failure criterion. This study presents a three-dimensional failure criterion for fiber-reinforced sand. By assuming that the total strength of the composite is a combination of the shear resistance of the host soil and the reinforcement of fibers, a general anisotropic failure criterion is proposed with special emphasis on the effect of isotropically/anisotropically distributed fibers. An anisotropic variable, defined by the joint invariant of the deviatoric stress tensor and a deviatoric fiber distribution tensor, is introduced in the criterion to quantify the fiber orientation with respect to the strain rate/stress direction at failure. With further consideration of the fiber concentration and other factors such as aspect ratio, the proposed criterion is applied to predicting the failure of fiber-reinforced sand in conventional triaxial compression/extension tests for both isotropically and anisotropically distributed fiber cases. The predictions are in good agreement with the test results available in the literature. The practical significance of using this criterion for such problems as inclined slope stabilization is briefly discussed. DOI: 10.1061/(ASCE)GT.1943-5606.0000737. © 2013 American Society of Civil Engineers.

CE Database subject headings: Fiber reinforced materials; Failures; Anisotropy; Triaxial tests; Slope stability; Sand (soil type).

Author keywords: Fiber-reinforced soil; Failure criterion; Anisotropy; Fiber distribution tensor; True triaxial tests; Slope stabilization.

Introduction

Earth reinforcement has become routine in geotechnical engineering to enhance the bearing capacity of geotechnical structures such as airfields, foundations, embankments, and pavement roads built on soft soils, and to stabilize engineered soil slopes and loosely filled retaining walls. Using fibers ranging from steel bars, polypropylene, polyester, glass fibers, and biodegradable fibers such as coir and jute, has been proven to be particularly effective for soil reinforcement (Santoni and Webster 2001; Liu et al. 2011). Some recent initiatives also use waste materials such as tire shred, waste fishing nets, and waster plastics as reinforcing fibers (Zornberg et al. 2004; Kim et al. 2008). Use of fiber reinforcement for soil improvement has been inspired by observations on the stabilizing effect of root systems to soils (Wu et al. 1979; Gray and Sotir 1995; Sonnenberg et al. 2010). Generally, the high tensile strength and extendibility of the added fibers help to effectively reduce the compressibility and brittleness of the host soil, which is generally superior to traditional soil improvement approaches such as using cement (Park 2011). Meanwhile, the reinforcing fibers can be placed either randomly to maintain strength isotropy or in a desired direction to provide optimal reinforcement.

The reliable design of fiber-reinforced soil structures requires a thorough understanding on the reinforcing mechanics and failure mechanisms. In particular, good prediction of the strength of the reinforced soil is of pivotal importance. Toward these goals, both laboratory tests and numerical simulations have been carried out.

Among the various experimental means, direct shear tests have been widely employed to simulate the pullout failure of fibers/roots along a shear band—like failure plane (Athanasopoulos 1996; Liu et al. 2009; Sadek et al. 2010). Meanwhile, being a proven way to explore soil behavior under a wide range of confining pressure, triaxial compression tests have been frequently used for the study of fiber-reinforced soils (Gray and Al-Refai 1986; Consoli et al. 2007b). Unconfined compression tests have also been employed to examine the strength of fiber-reinforced soil without lateral support (Kaniraj and Havanagi 2001). Numerical studies have also been carried out to investigate the behavior of fiber-reinforced soils (Sivakumar Babu et al. 2008). In general, the various approaches have shown that fiber inclusion can increase the peak strength as well as ductility of soil through the stretching of fibers and the mobilization of friction between the soil particles and fibers. A number of factors have been identified to be closely related to the efficiency of reinforcement, such as the fiber properties (length, density, aspect ratio, extendibility, and degradability of fiber), soil properties (gradation, particle size, shape, and density), effective confinement, and strain levels (Heineck et al. 2005; Consoli et al. 2007a; Liu et al. 2011).

A particularly distinct feature found in fiber-reinforced soils is the anisotropic behavior they may demonstrate under various loading conditions. This was first revealed by direct shear tests in which the measured strength of a fiber-reinforced soil was found to be dependent on the fiber orientation in the composite (Gray and Ohashi 1983; Jewell and Wroth 1987; Palmeira and Milligan 1989). More recent studies using triaxial compression and extension tests with varying fiber orientations have repeatedly supported the aforementioned observations (Li 2005; Diambra et al. 2010; Ibraim et al. 2010). For instance, Diambra et al. (2010) have shown that the contribution of fibers to soil strength is remarkable in triaxial compression but limited in triaxial extension, and have indicated that it is attributable to the preferred orientation of fibers in the tested samples (Diambra et al. 2007). The majority of fibers that align to the horizontal direction will experience tension in triaxial compression and can contribute considerably to the strength of the composite, whereas those fibers will mostly be subjected to compression under triaxial extension and therefore cannot fully unleash their enhancement to

¹Ph.D. Candidate, Dept. of Civil and Environmental Engineering, Hong Kong Univ. of Science and Technology, Clear Water Bay, Kowloon, Hong Kong SAR, China.

²Assistant Professor, Dept. of Civil and Environmental Engineering, Hong Kong Univ. of Science and Technology, Hong Kong SAR, China (corresponding author). E-mail: jzhao@ust.hk

Note. This manuscript was submitted on September 13, 2011; approved on March 20, 2012; published online on March 22, 2012. Discussion period open until June 1, 2013; separate discussions must be submitted for individual papers. This paper is part of the *Journal of Geotechnical and Geoenvironmental Engineering*, Vol. 139, No. 1, January 1, 2013. ©ASCE, ISSN 1090-0241/2013/1-95–106/\$25.00.

the composite strength (Michalowski and Čermák 2002; Michalowski 2008; Diambra et al. 2010).

In modeling the failure of fiber-reinforced soils, traditional approaches assume that the fiber orientation in the soil is random (Maher and Gray 1990; Zornberg 2002; Michalowski and Zhao 1996; Michalowski and Čermák 2003; Ranjan et al. 1996), while the real shear behavior of fiber-reinforced soil depends typically on the loading direction largely as a result of anisotropic fiber orientation. Traditional models apparently lead to inadequate characterization of the soil behavior. Recently, there have been a number of further improvements in this regard. For example, Michalowski and Čermák (2002) have employed a fiber distribution function to characterize the fiber orientation anisotropy and, hence, the anisotropic strength of the composite soil. The same approach has recently been employed by Diambra et al. (2010) in conjunction with the theory of mixture to model the strength and deformation anisotropy of fiber-reinforced sand. However, these latest developments have been limited to cases of plane strain or triaxial compression/extension conditions only, and may have difficulty in describing the failure of the composite soil under general three-dimensional (3D) loading conditions (e.g., the effect of both the intermediate principal stress magnitude and fiber distribution anisotropy). It is desirable to develop a general 3D failure criterion to describe the anisotropic strength of fiber-reinforced soils, which will be pursued in this paper. By assuming the composite strength is jointly contributed by the host soil and the fiber reinforcement, a failure criterion for the isotropic case of fiber distribution is formulated first. It will then be generalized to account for the strength anisotropy caused by the anisotropic fiber distribution. In doing so, a pivotal step is the introduction of an anisotropic variable, A , expressed by a joint invariant of the deviatoric stress tensor and the deviatoric fiber orientation tensor. This joint invariant enables describing the orientation of the fiber concentration with respect to the strain rate/stress direction at failure. A comparison between the predictions by the criterion and testing data in triaxial compression and extension is made, and their practical usefulness for geotechnical engineering problems is discussed.

Fiber Distribution Tensor and Anisotropic Variable

Fiber Distribution Tensor

Under external load, soil particles and fibers can form anisotropic internal structures that dictate the macroscopic deformation and failure of the composite soil. In modeling the anisotropic behavior of fiber-reinforced soil, it is of cardinal importance to choose a suitable quantity to characterize the internal structure. Generally, the internal structure depends on both the fabric structure of the host soil and the distribution of fibers. Recent experimental observations suggest that the anisotropic behavior of fiber-reinforced soil is dominated by the fiber orientation rather than by the host soil (Michalowski and Čermák 2002; Diambra et al. 2010). Hence, appropriate characterization of the fiber distribution becomes important, in which many past studies have employed a (scalar) function (Michalowski and Čermák 2002; Michalowski 2008; Diambra et al. 2010). However, a scalar description may not be adequate to characterize the spatial distribution of reinforcing fibers in the soil. A more general and robust way to describe the anisotropic behavior of fiber-reinforced soil in the 3D stress space would be tensor based. Indeed, fabric tensors have been widely employed to characterize the anisotropic internal structure comprised of particle contacts and void distribution in sand (Oda et al. 1985), and have also been used in the modeling of failure and deformation of geomaterials (Li and Dafalias 2002; Gao et al. 2010). In line with these studies, the following symmetric second-order tensor F_{ij} to

quantify the fiber distribution in a fiber-reinforced soil will be used (Oda et al. 1985):

$$F_{ij} = \frac{1}{V} \int_V \rho(\mathbf{n}) n_i n_j dV \quad (1)$$

where V = total volume of a representative volume element of the composite (see Fig. 1), n_i = i th component of the unit vector aligning in direction \mathbf{n} , and $\rho(\mathbf{n})$ = fiber concentration (ratio of fiber volume to composite volume) in direction \mathbf{n} (Michalowski and Čermák 2002). Ideally, $\rho(\mathbf{n})$ should be determined on a statistical basis within the representative element. Quite often, in both laboratory and engineering practice, the preparation techniques or the construction methods used lead to a distribution of fiber that can be largely regarded as cross anisotropic. In this case, a simplified fiber distribution function $\rho(\zeta)$ proposed by Michalowski and Čermák (2002) and used subsequently by Diambra et al. (2007) to characterize the fiber concentration may further be employed. Here, ζ is the angle of fiber inclination to the preferred fiber orientation plane (e.g., the x - y plane in Fig. 1). Importantly, both $\rho(\zeta)$ and $\rho(\mathbf{n})$ have to satisfy the following requirement (Michalowski and Čermák 2002):

$$\bar{\rho} = \frac{1}{V} \int_V \rho(\mathbf{n}) dV = \frac{1}{V} \int_V \rho(\zeta) dV = \frac{V_f}{V} \quad (2)$$

where $\bar{\rho}$ = average fiber concentration and V_f = total volume of fibers in the entire representative volume element shown in Fig. 1. The fiber concentration can also be described by the ratio between the weight of the fibers and that of the total composite soil (Maher and Gray 1990).

Fiber distribution tensor F_{ij} defined in Eq. (1) can always be decomposed into isotropic and deviatoric parts as follows:

$$F_{ij} = \frac{1}{3} \bar{\rho} (\delta_{ij} + d_{ij}) \quad (3)$$

where d_{ij} = deviatoric fiber distribution tensor, which contains information about the 3D distribution of fibers and the corresponding degree of anisotropy, and δ_{ij} = Kronecker delta (where $\delta_{ij} = 1$ for $i = j$ and $\delta_{ij} = 0$ for $i \neq j$). As noticed by Diambra et al. (2007), the moist tamping method that is frequently used in sample preparation in the laboratory typically produces a cross-anisotropic fiber distribution. Because the rolling and compaction processes are usually one-dimensional in engineering practice, a cross-anisotropic fabric distribution is also expected (Michalowski 2008). In doing so, it is assumed that the principal axes of fiber distribution tensor F_{ij} are aligned with the reference coordinate system (x, y, z), with the x - y

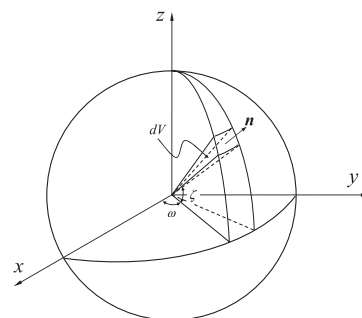


Fig. 1. Spherical representative volume element for fiber-reinforced soils (adapted from Michalowski and Čermák 2002)

plane being the isotropic plane (or the preferred fiber orientation plane), and z being directed to the axis of the cross anisotropy, which is the compacting direction. Eq. (3) can then be rewritten in the following matrix form:

$$F_{ij} = \begin{bmatrix} F_z & 0 & 0 \\ 0 & F_x & 0 \\ 0 & 0 & F_y \end{bmatrix} = \frac{1}{3}\bar{p} \begin{bmatrix} 1 & 0 & 0 \\ 0 & 1 & 0 \\ 0 & 0 & 1 \end{bmatrix} + \frac{1}{3}\bar{p} \begin{bmatrix} -\Delta & 0 & 0 \\ 0 & \Delta/2 & 0 \\ 0 & 0 & \Delta/2 \end{bmatrix} \quad (4)$$

where Δ = scalar that characterizes the magnitude of the cross anisotropy. Its value ranges from -2 when all the fibers align in the z direction ($F_z = \bar{p}$, $F_x = F_y = 0$) and 1 when there is no fiber aligning in the z direction [$F_z = 0$, $F_x = F_y = (1/2)\bar{p}$]. If $\Delta = 0$ [$F_x = F_y = F_z = (1/3)\bar{p}$], the fiber orientation is isotropic (random) in the 3D space.

Definition of an Anisotropic Variable

Michalowski and Čermák (2002) and Diambra et al. (2010) have found that only the portion of fibers that are subjected to tensile stress contribute to the strength of the composite soil. To describe this feature, it is important that a quantity can be defined to characterize the fiber concentration with respect to the loading direction. The strain rate axes direction has been employed by Michalowski and Čermák (2002) and Diambra et al. (2010) for such a purpose. However, it is sometimes not that convenient to determine the strain rate axes direction. In contrast, the stress is an easier quantity to measure and a convenient variable to use for a similar purpose. Indeed, at the failure stage of soil, the strain rate has been found to be largely coaxial with the applied stress for clean sand, even though the two are not coaxial at the early stage of loading (Gutierrez and Ishihara 2000). Although no testing results are yet available on fiber-reinforced soils in general 3D stress space, it is expected that the coaxial response at failure also holds under more general loading conditions, at least in an approximate sense. Based on the previous consideration, the following stress direction l_{ij} is employed to replace the strain rate direction in the study:

$$l_{ij} = \frac{S_{ij}}{\sqrt{S_{mn}S_{mn}}} \quad (5)$$

where $S_{ij} = \sigma_{ij} - p\delta_{ij}$ = deviatoric part of stress tensor σ_{ij} , and $p = \sigma_{mm}/3$ = mean stress. Furthermore, the following anisotropic variable A , which is used to characterize the fiber concentration with respect to the strain rate/loading direction at failure, is introduced:

$$A = \frac{l_{ij}d_{ij}}{\sqrt{d_{kl}d_{kl}}} \quad (6)$$

As can be seen from Eq. (6), a greater value of A indicates that fibers are oriented more preferably in the major principal stress direction, which is positive in compression. This implies that more fibers are being subjected to compression, and hence the reinforcing effect of the fibers to the composite strength is less efficient. For the case of a cross-anisotropically distributed fiber with the preferred fiber orientation plane being horizontal, the value of A is -1 in triaxial compression with the major principal stress being in the vertical direction, and $A = 1$ in triaxial extension with the major principal stress in the horizontal direction. For other general loading conditions, A varies between -1 and 1 . A detailed discussion of the change of A

with loading directions with respect to the cross-anisotropy plane can be found in Gao et al. (2010). Here, $A = 0$ for the isotropic fiber distribution case. Evidently, in addition to A , the degree of fiber distribution anisotropy $d = \sqrt{d_{ij}d_{ij}}$ also affects the strength anisotropy of fiber-reinforced soil and needs to be considered toward a realistic failure criterion, which will be discussed subsequently.

Failure Criteria for Fiber-Reinforced Sand

In line with previous studies (Gray and Ohashi 1983; Maher and Gray 1990; Zornberg 2002; Diambra et al. 2010), it is assumed that the shear strength of a fiber-reinforced soil is jointly attributed to by two parts, one from the host soil and the other by the fiber reinforcement. Furthermore, it is assumed that the anisotropy of the host soil is regarded as negligible compared with that induced by the reinforcing fibers, such that the host soil can be considered to be isotropic, while the reinforcing fibers dominate the anisotropic behavior of the composite strength. This assumption is also consistent with early studies by Michalowski (2008) and Diambra et al. (2010). Depending on the preparation method, the fibers can be distributed in the soil isotropically or anisotropically. The isotropic fiber distribution case will be discussed first and then the anisotropic case will be discussed.

Failure of Fiber-Reinforced Sand Considering the Isotropic Fiber Distribution

For a clean or cemented soil under general loading conditions, it is common to use the following description to characterize the soil strength (Yao et al. 2004):

$$q = M_c g(\theta)(p + \sigma_0^u) \quad (7)$$

where $q = \sqrt{3/2} s_{ij} s_{ij}$ = deviatoric stress; M_c = stress ratio q/p at failure in triaxial compression; σ_0^u = triaxial tensile strength of the soil without fiber reinforcement (see Fig. 2); and $g(\theta)$ = interpolation function characterizing the influence of the intermediate major principal stress magnitude on the failure of soils with θ being the Lode angle

$$\theta = \tan^{-1} \left(\frac{2b-1}{\sqrt{3}} \right) \quad (8)$$

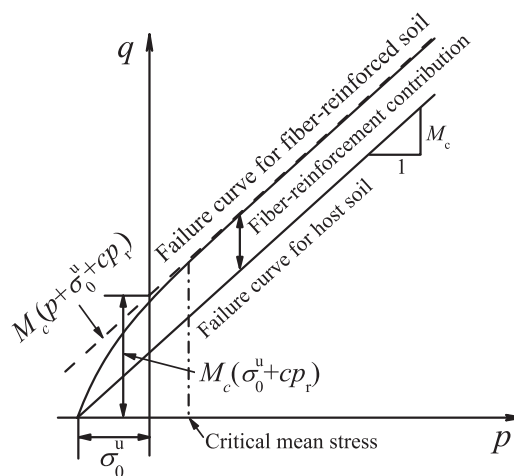


Fig. 2. Failure curves for unreinforced soil and fiber-reinforced soil in triaxial compression

where $b = (\sigma_2 - \sigma_3)/(\sigma_1 - \sigma_3) =$ intermediate principal stress ratio; $\sigma_1, \sigma_2,$ and $\sigma_3 =$ major, intermediate, and minor principal stress, respectively; and $g(\theta)$ is used to control the shape of the failure curves of soils (assumed to be isotropic here) in the deviatoric plane. In the current study, the following expression for $g(\theta)$ is employed (Sheng et al. 2000):

$$g(\theta) = \left[\frac{2\alpha^4}{1 + \alpha^4 + (1 - \alpha^4)\sin 3\theta} \right]^{1/4} \quad (9)$$

where $\alpha = M_e/M_c$ and $M_e =$ failure stress ratio q/p obtained in triaxial extension tests on the host soil. Evidently, with the expression in Eq. (9), $g(\theta)$ reaches a value of unity in triaxial compression and α reaches a value of unity in triaxial extension.

A failure criterion for fiber-reinforced sand can be developed based on Eq. (7). It is desirable to have a failure criterion accounting for the following two features under triaxial compression. (1) As the effective confinement $(p + \sigma_0^u)$ decreases, the failure envelope of fiber-reinforced soil converges to that of the host soil. The failure of the composite soil has been found to be governed by slip between soil particles and fibers at low confining pressure (Michalowski and Zhao 1996; Zornberg 2002; Consoli et al. 2007c). While the interface between the two is governed by frictional resistance, the fiber reinforcement will decrease with the decrease of effective confinement. At the extreme case of zero effective confinement $(p + \sigma_0^u = 0)$, the strength of the composite and the fiber reinforcement will both become zero. (2) The failure curve for the fiber-reinforced soil approaches a straight line with a slope of M_c at high effective confinement. At high effective confinement, the failure of the composite is expected to be mainly governed by either the yielding of the fiber (strong and thick fibers) or by fiber breaking (weak or very thin fibers) (Maher and Gray 1990; Consoli et al. 2007c; Michalowski 2008; Silva Dos Santos et al. 2010). In either of the two cases, the fiber reinforcement would reach a maximum/limit, which renders the failure envelopes for the reinforced and unreinforced soils parallel to each other at high confining pressure.

A simple bilinear relationship has been employed by Maher and Gray (1990) and Zornberg (2002) to describe the failure behavior of fiber-reinforced soil, wherein the two line segments intersect with each other at the critical confining/normal stress. Michalowski and Čermák (2003) considered various mechanisms of work dissipation at low and high confining pressures and proposed a criterion with a straight segment when the confining stress is below the critical confining stress and a curved one when it is above the critical confining stress. In this study, the following continuous functions is proposed to characterize the failure envelopes:

$$q = M_c g(\theta) [(p + \sigma_0^u) + f_c] \quad (10a)$$

$$f_c = cp_r \left[1 - \exp\left(-\kappa \frac{p + \sigma_0^u}{p_r}\right) \right] \quad (10b)$$

where c and $\kappa =$ two nonnegative material constants, $p_r =$ reference pressure (the atmospheric pressure, $p_{atm} = 101$ kPa, is adopted here), and $f_c =$ function describing the fiber reinforcement to the composite strength. Fig. 2 is an illustration of the failure criterion. It can be observed that the proposed criterion satisfies the two features previously mentioned. The predicted composite strength is zero at zero effective confinement state $(p + \sigma_0^u = 0)$, and the failure envelope approaches $q \approx M_c [(p + \sigma_0^u) + cp_r]$ when p is extremely large with $\kappa > 0$. When c and/or κ are zero, it leads to recovering the predicted failure curve for fiber-reinforced sand to that of the unreinforced soils [Figs. 3(a and b)]. Dimensionless constant c can be used to

characterize the maximum/limit fiber reinforcement in conjunction with p_r , because the maximum value of f_c is cp_r according to Eq. (10b) [see also Fig. 2 and Fig. 3(a)]. Following Maher and Gray (1990) and Zornberg (2002) as well as Michalowski and Čermák (2003), the mean stress at which the failure curve reaches the straight part will be termed the critical mean stress. The value of κ controls the magnitude of this critical mean stress beyond which the failure of fiber-reinforced soils would be governed by either fiber yielding or breakage because a higher value of κ renders the failure curve to approach the straight segment at a relatively lower mean stress level, as shown in Fig. 3(b). Both c and κ may depend on the fiber property, soil property, and frictional characteristics between fibers and soil.

The term accounting for the fiber-reinforcement contribution in Eq. (10b), f_c , has the same form as sliding function f_b proposed by Diambra et al. (2010), where f_b has been used by Diambra et al. (2010) to characterize the bonding efficiency between sand particles and fibers when $p = 0$ and $f_b = 0$ (full sliding); f_b reaches a positive limit value at very high confining pressure. It can be expected that the fiber reinforcement would be approximately proportional to f_b as long as the fibers are intact. Therefore, to some extent function f_c can

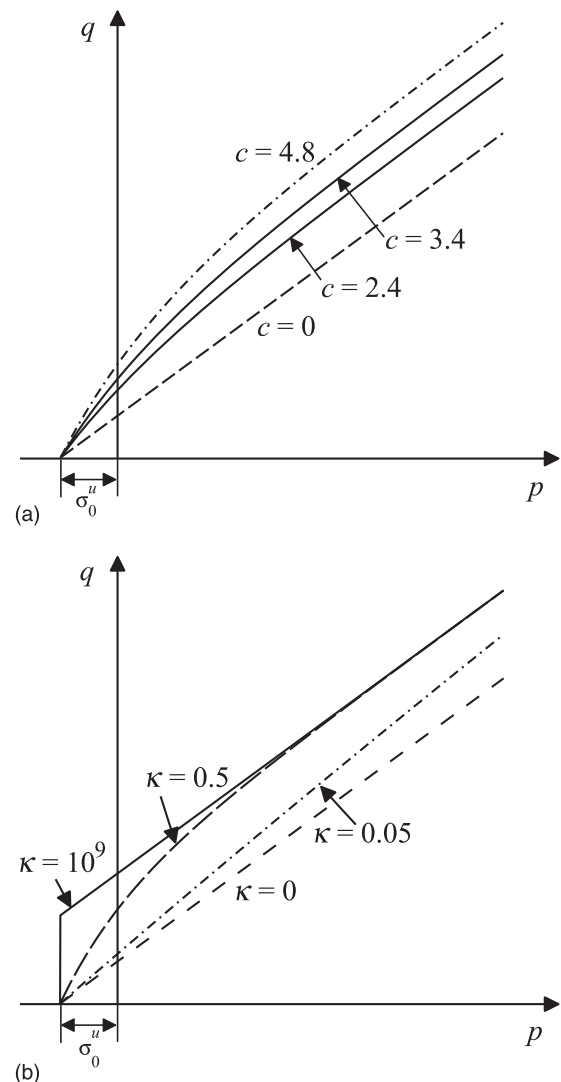


Fig. 3. Illustration of the effect of parameters (a) c and (b) κ on the criterion predictions

also be treated as a measure of the bonding efficiency between the soil particles and fibers.

To verify the proposed failure criterion in Eq. (10), a comparison will be made between its predictions on the shear strength for fiber-reinforced sand with random fiber orientation under triaxial conditions and the test data. It is helpful to first briefly introduce the parameter calibration. Parameters M_c and σ_0^u can be readily calibrated according to the test results on the host soil without fiber. As can be seen from Fig. 2, the intersection of the dashed line (which merges to the straight portion of the failure curve of the fiber-reinforced soils at a high mean stress level) with the q axis is $M_c(\sigma_0^u + cp_r)$, which can be used to determine the value of c in conjunction with of the already known M_c and σ_0^u . Finally, parameter κ can be calibrated through trial and error. Experience has shown that a typical value of κ in the range of 0.0–0.7 is acceptable. For the triaxial compression case, $g(\theta) = 1$.

Shown in Fig. 4 are two sands reinforced by glass fiber tested by Maher and Gray (1990), the Muskegon Dune sand and mortar sand. The glass fiber concentration in both sands is around 3% by weight but with various aspect ratios (defined as the ratio between the fiber length and diameter). For either case, various κ have been obtained. Nevertheless, it is found that the variation of κ with the fiber aspect ratio is small, and a single value of κ suits fairly well for either sand case. It is found that the value of c generally increases with the aspect ratio of the glass fiber, which is consistent with the regressed relationship obtained by Ranjan et al. (1996). At the same fiber aspect ratio, the value of c is found to be greater for fiber-reinforced Muskegon Dune sand than for fiber-reinforced mortar sand, while the κ value is greater for the latter sand. Several factors—such as gradation, particle shape, and grain size—are attributable to the observed differences (Maher and Gray 1990). From Fig. 4 notably good agreement between the prediction by the proposed failure criterion and the testing data can be observed in both sand cases.

The failure criterion in Eq. (10) has also been used to predict the strength of chopped polypropylene fiber-reinforced/unreinforced nonplastic silty-sand reported by Heineck and Consoli (2004). The fiber content for this case is 0.5% by weight. The prediction and comparison are presented in Fig. 5. Overall, the prediction agrees well with the test data for this sand, too. Also, with a critical mean stress for this sand at a much lower 250 kPa than the previous two sands (around 500–750 kPa), the value of κ for this case is greater than for the former two cases. This may have been caused by the use of a much smaller diameter and lower concentration of fiber in this case than in the previous two cases. The fiber aspect ratio for this case is also much higher than in the former two cases, which will yield a lower critical confining stress. This is consistent with the observation by Michalowski and Čermák (2003) as well.

Failure Criterion for Fiber-Reinforced Sand with the Anisotropic Fiber Distribution

Based on Eq. (10) and the fact that the strength anisotropy of fiber-reinforced sand is dominated by the anisotropic fiber distribution, the following expression is proposed to describe the strength anisotropy of fiber-reinforced sand by assuming that the fiber reinforcement depends on anisotropic variable A and the degree of fiber distribution anisotropy d

$$q = M_c g(\theta) \left\{ (p + \sigma_0^u) + \tilde{c}(A) p_r \left[1 - \exp\left(-\kappa \frac{p + \sigma_0^u}{p_r}\right) \right] \right\} \quad (11)$$

where

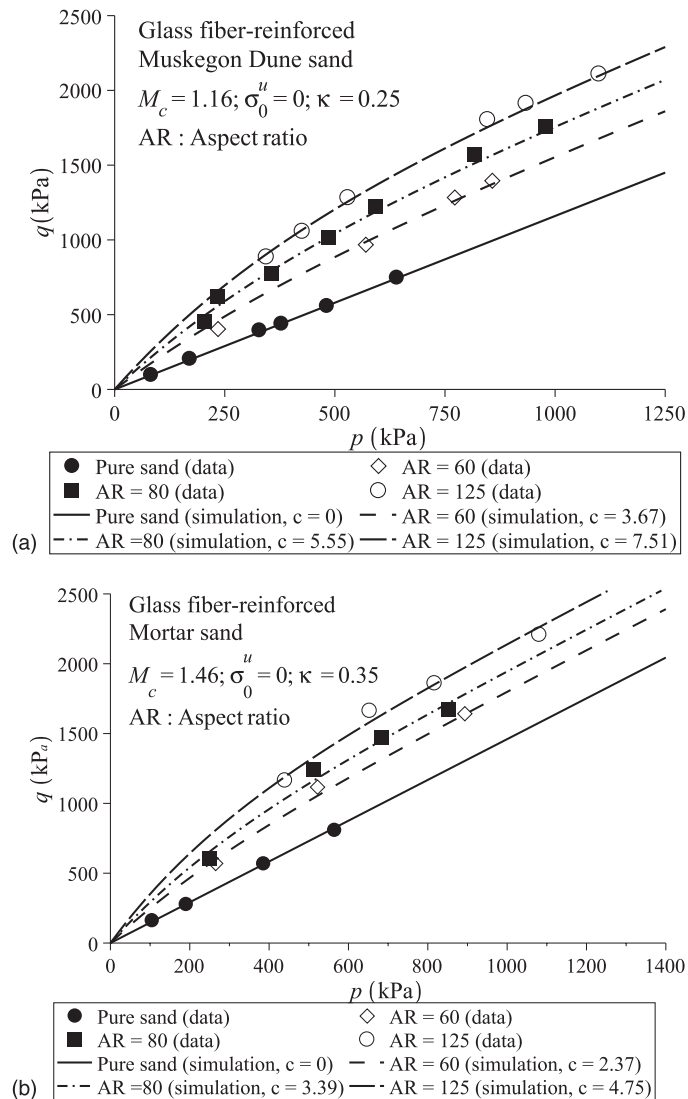


Fig. 4. Comparison between the prediction of the proposed failure criterion and the test results on two glass fiber-reinforced sands (fiber concentration at 3% by weight and various aspect ratios): (a) Muskegon Dune sand and (b) Mortar sand (data from Maher and Gray 1990)

$$\tilde{c} = ce^{\lambda d}(1 - \psi A) \quad (12)$$

where λ and ψ two positive material parameters. Essentially, $e^{\lambda d}$ in Eq. (12) is used to quantify the degree of strength anisotropy of fiber-reinforced sand. Because $-1 \leq A \leq 1$ and $\tilde{c} \geq 0$ should be satisfied, ψ should range from zero to unity. For special cases where fiber distribution tensor F_{ij} can be expressed in the form of Eq. (4) and Δ can be readily obtained [e.g., all fibers orient in the z direction ($\Delta = -2$) or all fibers evenly align in the x - y plane ($\Delta = 1$)], degree of anisotropy d is known and λ is a separate parameter. However, for most applications the preferred fiber distribution plane is known a priori (A can be calculated) while d is hard to determine. Thus, the entire term $e^{\lambda d}$ can be treated as one parameter and can be further calibrated against the test results with various loading directions. Indeed, $ce^{\lambda d}$ can even be taken as a single parameter when the fiber distribution is fixed and the test data with a random (isotropic) fiber distribution are not available (e.g., c cannot be obtained). Some interesting observations can be further made from Eqs. (11) and (12):

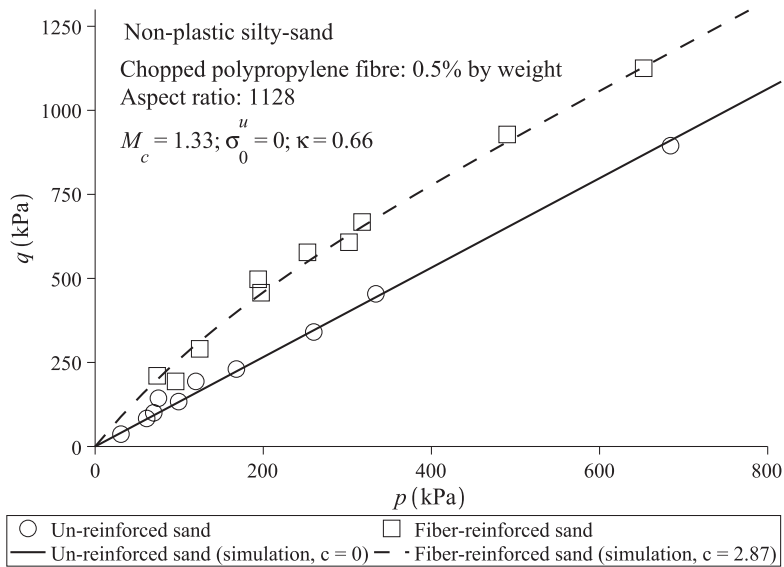


Fig. 5. Comparison between the criterion prediction and the test results for a fiber-reinforced/unreinforced nonplastic silty-sand (data from Heineck and Consoli 2004)

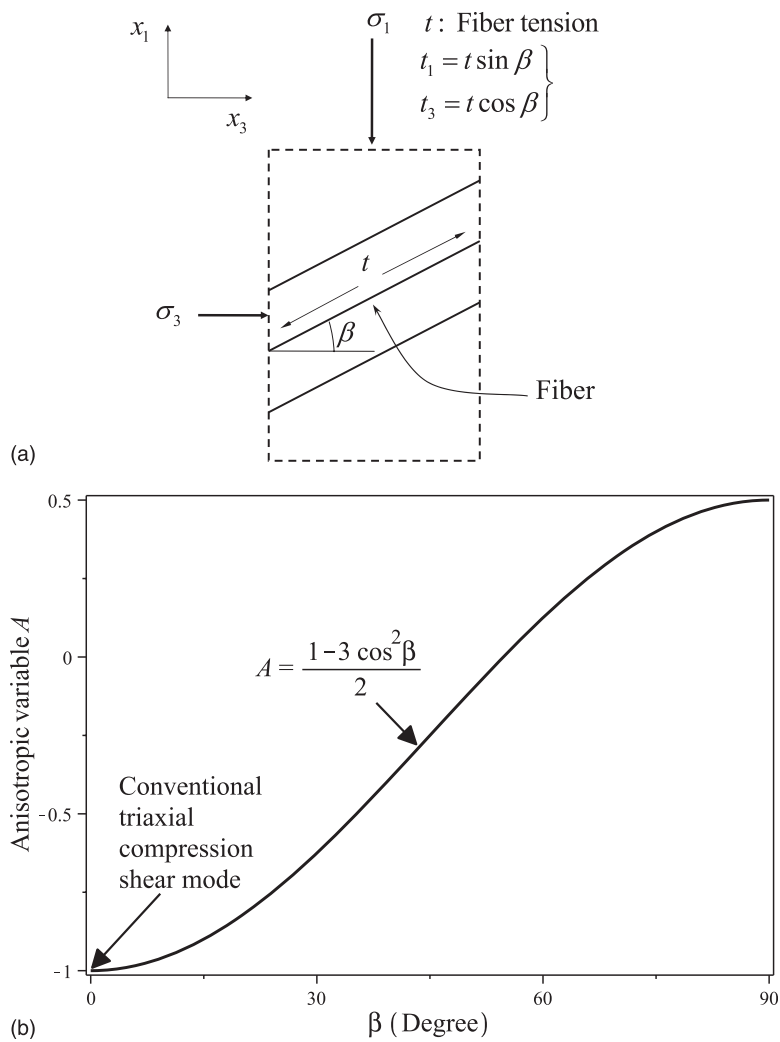
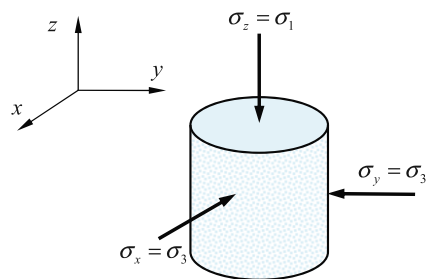


Fig. 6. Illustration of fiber-reinforcement anisotropy in triaxial compression with various preferred fiber orientations

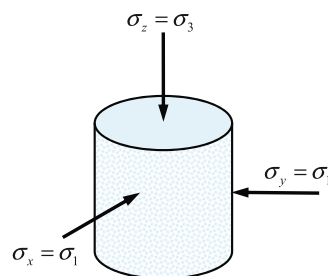
1. If the fiber distribution is isotropic, both d and A will become zero. Hence, $\tilde{c} = c$ and Eq. (11) becomes identical to Eq. (10). The isotropic case in Eq. (10) thus represents a special case of Eq. (11).
2. When the fiber distribution is anisotropic, $d > 0$, \tilde{c} will vary with A . As λ is typically positive, \tilde{c} also increases with the degree of anisotropy d .
3. If the fiber distribution is fixed, when the major principal stress direction deviates from the axis of the preferred fiber orientation plane, A increases and \tilde{c} decreases. Physically, such a change implies that there will be more fibers tending to align in the major principal stress direction and becoming more subjected to compression, which essentially renders the reinforcing of fibers less effective. A simple illustration is given in Fig. 6 of this mechanism in triaxial compression, wherein all fibers are supposed to orientate in one preferred plane with an angle of β to the horizontal. Evidently, only the horizontal component t_3 ($=t \cos \beta$) of total fiber tension t contributes to the reinforcement by preventing lateral expansion of the sample. As can be seen from Fig. 6(b), the reinforcing effect will generally decrease with an increasing β , or with an increasing A . This phenomenon has already been experimentally confirmed by Michalowski and Čermák (2002) and Diambra et al. (2010).
4. Eq. (12) can also be used in conjunction with other isotropic failure criteria to account for strength anisotropy. For instance, the cohesion c_{MC} and/or the friction angle φ_{MC} in the Mohr-Coulomb (MC) failure criterion can be assumed to be functions of A and d to model the strength anisotropy of fiber-reinforced soils.

Prediction of the Strength Anisotropy for Fiber-Reinforced Sand

Michalowski and Čermák (2002) have carried out a series of triaxial compression tests on fiber-reinforced sand with various fiber orientations. Three cases of fiber orientation have been tested, including random, purely horizontal, and purely vertical-orientated fibers [see Fig. 7(a)]. Relevant to these cases, the anisotropic variables involved in Eq. (11) (Δ , d , and A) can be readily determined, as given in



(a) Triaxial compression



(b) Triaxial extension

Fig. 7(a). Before Eq. (11) is applied to the prediction of these cases, it is instructive to explain how the model parameters are calibrated. First, M_c and σ_0^u are obtained based on the test results on unreinforced sand in conjunction with Eq. (7) [$g(\theta) = 1$]. Because no fibers were observed by Michalowski (1996) to yield at the tested pressure level, a small value of $\kappa = 0.05$ was selected according to the parametric study in Fig. 3(b). Parameter c was then adjusted to fit the test data with the random fiber orientation [Eq. (10)]. Considering the mechanism mentioned previously, it was assumed that the reinforcing effect was zero for the vertical fiber distribution case ($A = 1$), in which $\psi = 1$ can be determined according to Eq. (12). Finally, λ was calibrated through fitting the test data with the horizontal fiber distribution case in conjunction with Eqs. (11) and (12). Shown in Fig. 8(a) is the comparison between the triaxial compression test results and the predictions by Eq. (11) as well as the calibrated parameters.

Although there are no data available, the predictions on the triaxial extension case are also provided using the same set of parameters in Fig. 8(b). The corresponding values for Δ , d , and A are shown in Fig. 7(b), where $\alpha = 0.75$ was chosen according to Li and Dafalias (2002). Evidently, the fiber reinforcement is greater in the vertical fiber distribution case ($A = -1$), while it appears to be negligibly small in the horizontal fiber distribution case ($A = 1$). Indeed, Li (2005) conducted two sets of triaxial extension tests on fiber-reinforced sand with horizontally and vertically preferential planes of fiber orientation [similar to the cases shown in Fig. 7(b)]. The composite strength was found to be much higher in the latter case, which is consistent with the predictions by the current proposed criterion. However, because the fiber concentration is relatively small and the available data points are scarce in Michalowski and Čermák (2002), further tests with more data would definitely lend more confidence to the proposed criterion.

Prediction of the True Triaxial Failure Strength for Fiber-Reinforced Sand

True triaxial tests have been widely used to investigate the effect of intermediate principal stress and fabric anisotropy on the behavior of soils in general 3D stress space (Kirkgaard and Lade 1993).

i) Random fiber distribution:

$$\Delta=0, d=0, A=0$$

ii) Purely horizontal fiber distribution:

$$\Delta=1, d=\sqrt{1.5}, A=-1$$

iii) Purely vertical fiber distribution:

$$\Delta=-2, d=\sqrt{6}, A=1$$

i) Random fiber distribution:

$$\Delta=0, d=0, A=0$$

ii) Purely horizontal fiber distribution:

$$\Delta=1, d=\sqrt{1.5}, A=1$$

iii) Purely vertical fiber distribution:

$$\Delta=-2, d=\sqrt{6}, A=-1$$

Fig. 7. Illustration of the triaxial compression and extension test conditions and corresponding values of the relevant anisotropic variables

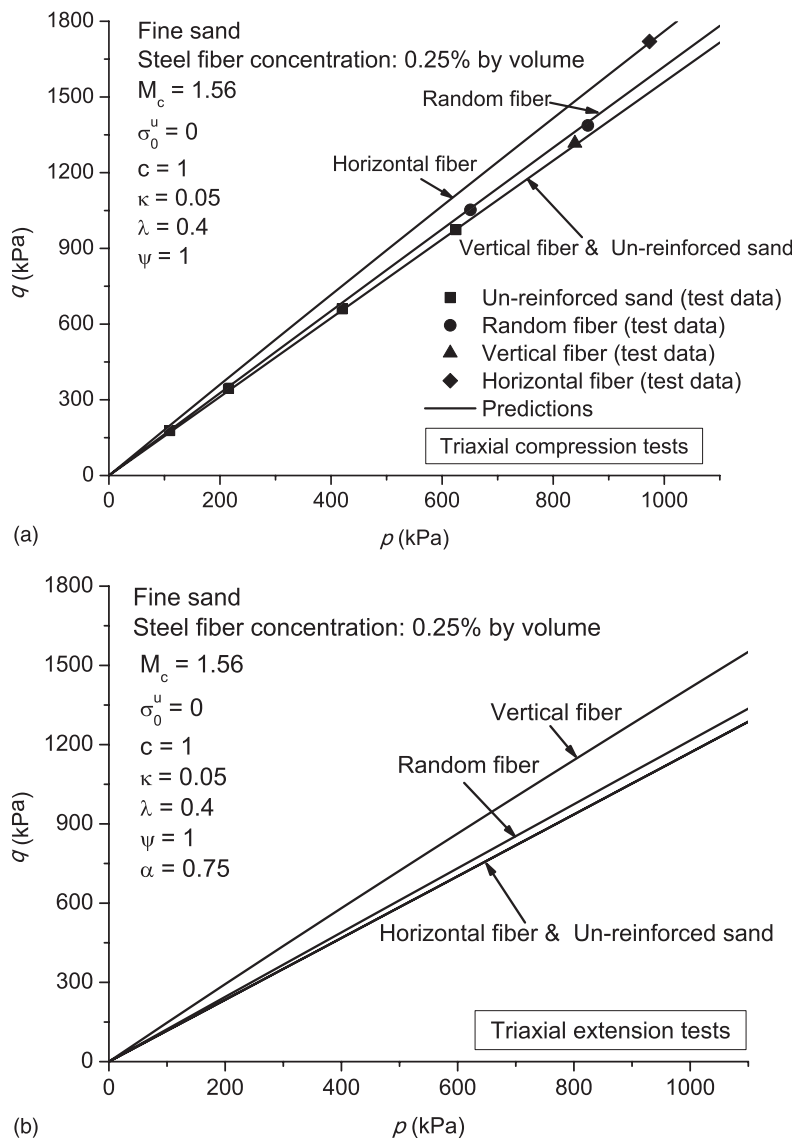


Fig. 8. (a) Comparison between the predictions of the proposed failure criterion on the strength anisotropy of fiber-reinforced sand with the test data by Michalowski (1996) and Michalowski and Čermák (2002) and (b) predictions by the proposed failure criterion for the triaxial extension case

However, very few true triaxial tests on fiber-reinforced soils have been done, thus a comparison cannot be made between the criterion predictions and test data here. Nevertheless, the proposed failure criterion expressed by Eqs. (11) and (12) has been used to predict the strength of fiber-reinforced soils under typical true triaxial tests with the loads being applied as shown in Fig. 9. In performing these predictions, it is assumed that the fiber orientation in the composite is either isotropic or cross anisotropic with the preferred fiber orientation plane being horizontal. For the relationship between $\tilde{\theta}$ and b in Fig. 9(a), the reader is referred to Kirkgaard and Lade (1993).

In selecting the values of relevant parameters, it is first assumed that under triaxial extension, $\tilde{c} = 0$. This is indeed supported by the observations by Diambra et al. (2010) and Ibraim et al. (2010). At this special shear mode, $\tilde{\theta} = 180^\circ$ [Fig. 9(a)] and $A = 1$ [Fig. 9(b)], $\psi = 1$ may be assumed according to Eq. (12). The values of M_c , c , λ , κ , and α are chosen in the range of those parameters discussed in the previous subsection; where $c = 0$ is used for the case of unreinforced soil. The predictions are shown in the deviatoric plane [Fig. 9(c)] and in the 3D stress space [Fig. 9(d)],

respectively. It is evident that the fiber reinforcement can enlarge the failure surface evenly in the deviatoric plane for the isotropic fiber distribution case ($\Delta = 0$), which indicates that the isotropic fiber distribution can maintain the strength isotropy of the composite and prevent the development of weak areas. As for the anisotropic fiber distribution cases frequently encountered in laboratory and engineering practice, both Figs. 9(c and d) indicate that the reinforcing effect is strongly related to the stress direction. As is seen in Fig. 9(c), the fiber reinforcement leads to a maximum shear strength for the composite soil at $\tilde{\theta} = 0^\circ$ and a minimum at $\tilde{\theta} = 180^\circ$. As $\tilde{\theta}$ increases from 0 to 180° , the value of A increases from its minimum of -1 to its maximum of 1 [Fig. 9(b)]. Physically, this implies that the major principal stress direction tends to change gradually from the perpendicular direction of the preferred fiber orientation plane to one that aligns with it more, which naturally leads to a decrease of the reinforcing efficiency for the fibers. As Δ increases from 0 to 1, the degree of fiber anisotropy d increases from 0 to $\sqrt{1.5}$ and \tilde{c} also increases at $\tilde{\theta} = 0$ according to Eq. (12) ($A \equiv 1$ with positive Δ in this mode). The physical significance is that more fibers tend to orient in the horizontal plane and the fiber reinforcement

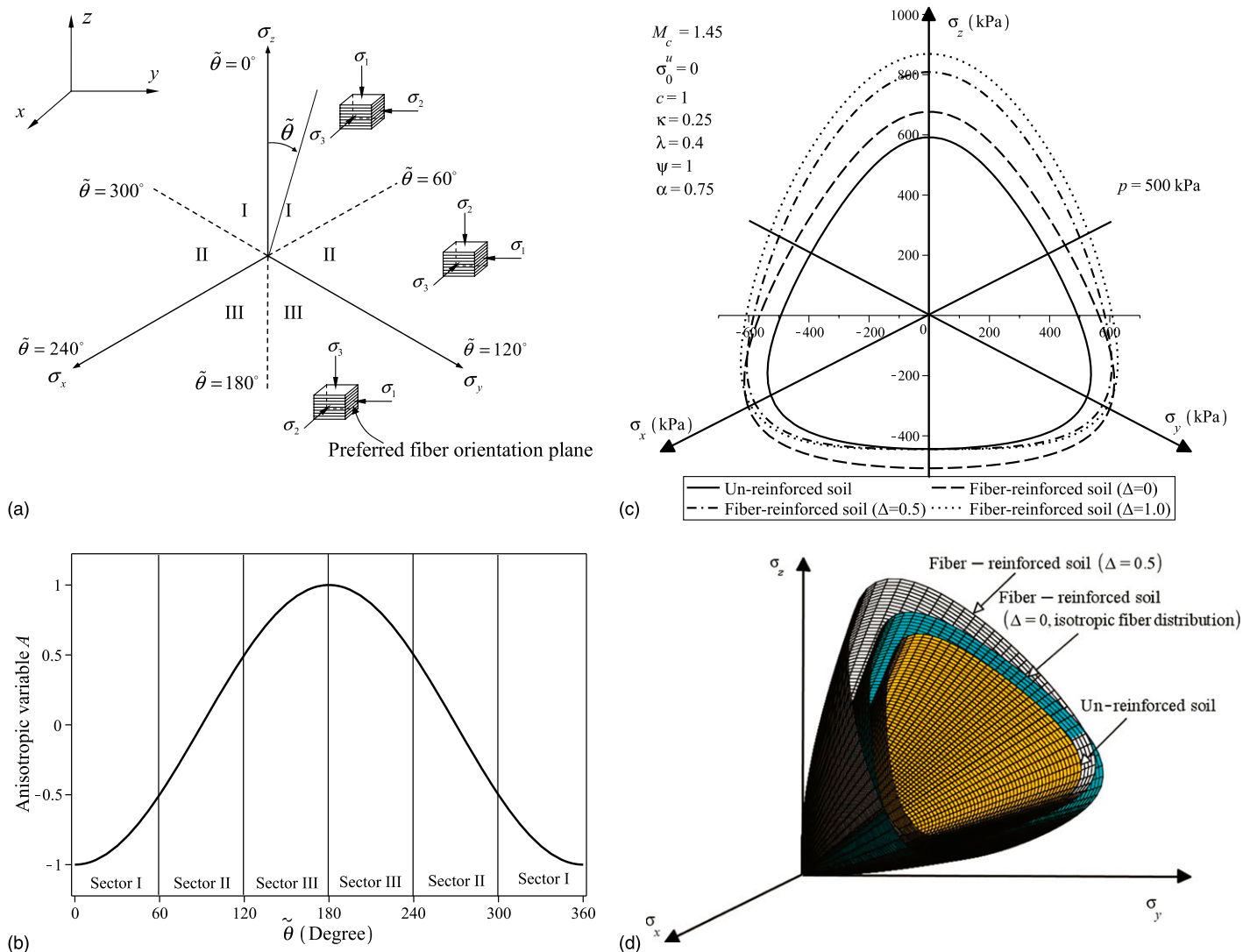


Fig. 9. (a) Loading conditions in the true triaxial tests (adapted from Kirkgaard and Lade 1993); (b) variation of anisotropic variable A with $\tilde{\theta}$ with $0 < \Delta \leq 1$; (c) prediction of the failure criterion in Eq. (11) in the deviatoric plane; and (d) in the 3D stress space

increases in this conventional triaxial compression shear mode. Accordingly, the variation of strength with A also increases [Eq. (12)].

Relevance to Practical Applications

Fiber reinforcement is commonly used in the stabilization of soil slopes (Gregory and Chill 1998). Because the reinforcing effect is strongly dependent on the relative orientation between the loading direction and the preferred fiber orientation, special attention should be paid to how to place the fibers in an optimal way during construction. In this connection, the proposed failure criteria may serve as a useful tool for the analysis. The example of a homogeneous slope with a potential slip surface shown in Fig. 10(a) can be taken as an illustration. It is assumed that the slope is long enough in the out-of-plane direction in which intermediate principal stress σ_2 aligns. The preferred fiber orientation plane is further assumed to be parallel to the out-of-plane direction. The stress state for a soil element along the failure surface at various depths can then be described by the angle between the major principal stress direction and the vertical direction, ξ , as well as intermediate principal stress variable b (Hwang et al. 2002; Zdravković et al. 2002; Shogaki and Kumagai 2008). For

the convenience of discussion, it is further assumed that the soil property, fiber property, and concentration are known and the b value, as well as mean stress p at each location, is determined according to the slope geometry and soil density. As a result, only variable A affects the reinforcing effect of the fiber at each location according to Eqs. (11) and (12). A general soil element as shown in Fig. 10(b) may be taken to facilitate the analysis, where β is the angle between the major principal with the normal direction of the preferred fiber orientation plane [Fig. 10(b) is essentially a 3D view of the element in Fig. 6(a) when $b = 0$]. In this case, A can be simplified as (Gao et al. 2010)

$$A = \frac{3 \sin^2 \beta + b - 2}{2\sqrt{b^2 - b + 1}} \quad (13)$$

The variation of A with b and β is plotted in Fig. 10(c). When all the other variables are fixed, the strength of the composite is reversely proportional to A according to Eqs. (11) and (12). While from Eq. (13), when the major principal stress direction is perpendicular to the preferred fiber orientation plane at each critical location of the slip surface, A is a minimum, and thus the fiber reinforcement can be optimally achieved. That is, when $\beta = 0^\circ$, the enhancement of

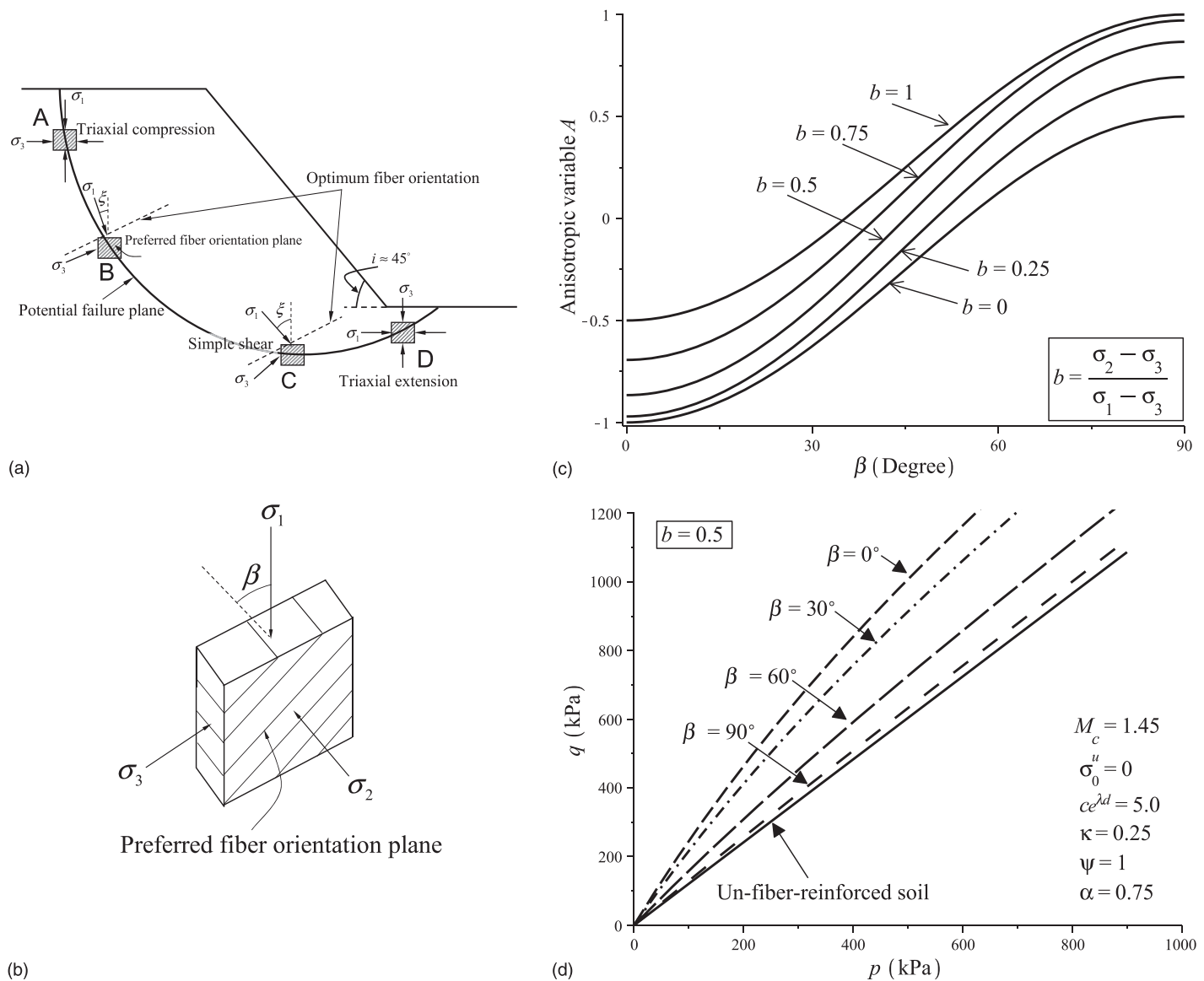


Fig. 10. (a) Orientation of the major principal stress direction on the potential failure plane in a homogeneous soil slope (adapted from Uthayakumar and Vaid 1998); (b) relative orientation between the major principal stress direction and preferred fiber distribution plane β ; (c) variation of anisotropic variable A with β at various intermediate principal stress variables; (d) predicted anisotropic strength varying with fiber orientation at $b = 0.5$

strength is most significant, whereas it is negligible at $\beta = 90^\circ$. This can be further demonstrated by the case of $b = 0.5$ in Fig. 10(d). However, in engineering practice it is difficult to place all fibers in such an optimum manner along the entire potential failure surface. A cost-effective, yet convenient, method is to place the fibers along the same orientation according to a certain critical spot along the slip surface, which may help to provide a relatively effective reinforcement, if not optimally. Numerical simulations by Hwang et al. (2002) indicate that such a critical location for a slope under investigation here is around Spot B in Fig. 10(a). Based further on the stress contour obtained by Zdravković et al. (2002) for a similar problem, it is suggested to choose an optimum fiber orientation in the range of 10° – 20° to the horizontal for a slope with an inclination of around 45° , as shown in Fig. 10(a). This range may change if the slope geometry and soil property vary. In an extreme case of vertical cut, when the major principal stress direction is close to the vertical along the potential failure plane, the fibers should be placed with a preferred orientation plane horizontal to achieve

maximum reinforcement. This is consistent with the conclusion made by Michalowski (2008).

Indeed, in the stabilization of inclined soil slopes using soil nails, a similar concept has been used. For example, Wei and Cheng (2010) simulated a similar problem and have shown that the optimum soil nail inclination is around 10° – 30° to the horizontal. Centrifuge tests by Tei et al. (1998) also demonstrated that using soil nails at around 10° of inclination to the horizontal provides more effective prevention of horizontal movement of the slope. In bio-technical slope stabilization, root orientation is also an important factor affecting the reinforcing efficiency (Gray and Ohashi 1983; Jewell and Wroth 1987; Sonnenberg et al. 2010). Direct shear tests by Gray and Ohashi (1983), Jewell and Wroth (1987), and Palmeira and Milligan (1989) have shown that the reinforcement is the maximum when fiber inclination ϑ_2 with respect to the vertical is around 30° (see Fig. 11). Recent distinct element simulations performed by Cui and O'Sullivan (2006) and Wang and Gutierrez (2010) have shown that the major principal stresses have an angle of

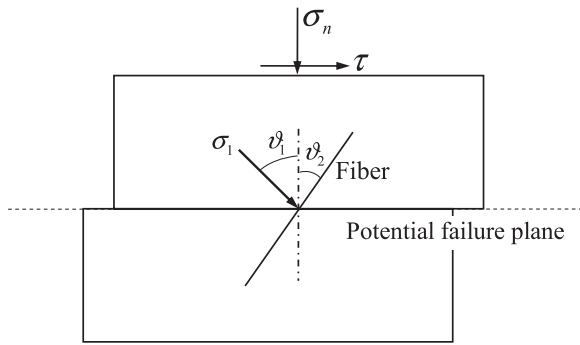


Fig. 11. Illustration of the direct shear test on fiber-reinforced soil and the major principal stress orientation around the sample center

$\vartheta_1 \approx 60^\circ$ relative to the vertical (Fig. 11). It can be seen readily that $\vartheta_1 + \vartheta_2 \approx 90^\circ$. This confirms the conclusion that the maximum reinforcement can be achieved when the major principal stress direction is perpendicular to the preferred fiber-orientation plane.

Conclusions

A 3D failure criterion is proposed for fiber-reinforced sand. By assuming the total composite strength is contributed from the shear resistance of the host soil and the fiber reinforcement, the criterion is first developed for the isotropic fiber distribution case. It is then generalized to the 3D stress space to account for the effect of anisotropic fiber distribution. An anisotropic variable A defined as a joint invariant of the deviatoric stress tensor and a deviatoric fiber distribution tensor is introduced to quantify the fiber concentration with respect to the strain rate/stress direction at failure. The strength of fiber-reinforced soils is formulated to be dependent on A as well as the degree of the fiber distribution anisotropy. The proposed criterion has been applied to predict the strength of fiber-reinforced sand with both isotropic and anisotropic fiber distributions, in triaxial compression/extension tests, and the predictions agree fairly well with the test data. Further predictions by the criterion for typical true triaxial tests have also been conducted. While the proposed failure criterion has been shown to be capable of offering reasonable characterization of the strength anisotropy for fiber-reinforced sand, its usefulness for practical application is further demonstrated by an example of homogeneous soil slope. The study may be a useful reference for other reinforcing approaches such in biotechnical means (e.g., through plant roots) and soil nails.

Acknowledgments

This work was supported by the Research Grants Council of Hong Kong (under Grant Nos. 623211 and SBI08/09.EG02).

Notation

The following symbols are used in this paper:

- A = anisotropic variable;
- b = intermediate principal stress parameter;
- c = parameter characterizing the maximum fiber reinforcement;
- c_{MC} = cohesion in the Mohr-Coulomb failure criterion;
- \tilde{c} = maximum fiber reinforcement accounting for anisotropy;
- d = degree of fiber distribution anisotropy;

- d_{ij} = deviatoric fabric distribution tensor;
- F_{ij} = fabric distribution tensor;
- f_b = function describing the bonding efficiency between sand particles and fibers;
- f_c = function for fiber reinforcement;
- $g(\theta)$ = interpolation function for the failure stress ratio;
- l_{ij} = stress direction tensor;
- M_c = failure stress ratio in triaxial compression;
- M_e = failure stress ratio in triaxial extension;
- p = mean stress;
- p_r = reference pressure;
- q = deviatoric stress;
- s_{ij} = deviatoric stress tensor;
- β = major principal stress direction;
- Δ = variable characterizing the fiber orientation anisotropy;
- δ_{ij} = Kronecker delta;
- θ = Lode angle of the stress tensor;
- $\tilde{\theta}$ = variable characterizing the stress state in true triaxial tests;
- κ = parameter controlling the magnitude of critical mean stress;
- λ = parameter characterizing the strength variation with the degree of fiber distribution anisotropy;
- ξ = major principal stress direction;
- $\rho(\mathbf{n})$ = fiber concentration function;
- $\bar{\rho}$ = average fiber concentration;
- σ_{ij} = stress tensor;
- σ_0^u = triaxial tensile strength of the host sand;
- $\sigma_1, \sigma_2, \sigma_3$ = major, intermediate, and minor principal stresses, respectively;
- φ_{MC} = friction angle in the Mohr-Coulomb failure criterion; and
- ψ = parameter characterizing the strength variation with the loading direction.

References

- Athanasopoulos, G. A. (1996). "Results of direct shear tests on geotextile reinforced cohesive soil." *Geotext. Geomembr.*, 14(11), 619–644.
- Consoli, N. C., Casagrande, M. D. T., and Coop, M. R. (2007a). "Performance of a fibre-reinforced sand at large shear strains." *Geotechnique*, 57(9), 751–756.
- Consoli, N. C., Foppa, D., Festugato, L., and Heineck, K. S. (2007b). "Key parameters for strength control of artificially cemented soils." *J. Geotech. Geoenviron. Eng.*, 133(2), 197–205.
- Consoli, N. C., Heineck, K. S., Casagrande, M. D. T., and Coop, M. R. (2007c). "Shear strength behavior of fiber-reinforced sand considering triaxial tests under distinct stress paths." *J. Geotech. Geoenviron. Eng.*, 133(11), 1466–1469.
- Cui, L., and O'Sullivan, C. (2006). "Exploring the macro- and micro-scale response of an idealised granular material in the direct shear apparatus." *Geotechnique*, 56(7), 455–468.
- Diambra, A., Ibraim, E., Muir Wood, D., and Russell, A. R. (2010). "Fibre reinforced sands: Experiments and modeling." *Geotext. Geomembr.*, 28(3), 238–250.
- Diambra, A., Russell, A. R., Ibraim, E., and Muir Wood, D. (2007). "Determination of fibre orientation distribution in reinforced sand." *Geotechnique*, 57(7), 623–628.
- Gao, Z. W., Zhao, J. D., and Yao, Y. P. (2010). "A generalized anisotropic failure criterion for geomaterials." *Int. J. Solids Struct.*, 47(22–23), 3166–3185.
- Gray, D. H., and Al-Refeai, T. (1986). "Behavior of fabric- versus fiber-reinforced sand." *J. Geotech. Eng.*, 112(8), 804–820.

- Gray, D. H., and Ohashi, H. (1983). "Mechanics of fiber reinforcement in sands." *J. Geotech. Engrg.*, 109(3), 335–353.
- Gray, D. H. and Sotir, B. (1995). "Biotechnical stabilization of steepened slopes." *Transportation Research Record 1474*, Transportation Research Board, Washington, DC, 23–29.
- Gregory, G. H., and Chill, D. S. (1998). "Stabilization of earth slopes with fiber-reinforcement." *Proc., 6th Int. Conf. on Geosynthetics*, Industrial Fabrics Association International, Atlanta, 1073–1078.
- Gutierrez, M., and Ishihara, K. (2000). "Non-coaxiality and energy dissipation in granular material." *Soils Found.*, 40(2), 49–59.
- Heineck, K. S., and Consoli, N. C. (2004). "Discussion of 'Discrete framework for limit equilibrium analysis of fibre-reinforced soil' by J. G. Zornberg." *Geotechnique*, 54(1), 72–73.
- Heineck, K. S., Coop, M. R., and Consoli, N. C. (2005). "Effect of microreinforcement of soils from very small to large shear strains." *J. Geotech. Geoenviron. Eng.*, 131(8), 1024–1033.
- Hwang, J., Dewoolkar, M., and Ko, H.-Y. (2002). "Stability analysis of two-dimensional excavated slopes considering strength anisotropy." *Can. Geotech. J.*, 39(5), 1026–1038.
- Ibraim, E., Diambra, A., Muir Wood, D., and Russell, A. R. (2010). "Static liquefaction of fibre reinforced sand under monotonic loading." *Geotext. Geomembr.*, 28(4), 374–385.
- Jewell, R. A., and Wroth, C. P. (1987). "Direct shear tests on reinforced sand." *Geotechnique*, 37(1), 53–68.
- Kaniraj, S. R., and Havanagi, V. G. (2001). "Behavior of cement-stabilized fiber-reinforced fly ash-soil mixtures." *J. Geotech. Geoenviron. Eng.*, 127(7), 574–584.
- Kim, Y. T., Kim, H. J., and Lee, G. H. (2008). "Mechanical behavior of lightweight soil reinforced with waste fishing net." *Geotext. Geomembr.*, 26(6), 512–518.
- Kirkgaard, M. M., and Lade, P. V. (1993). "Anisotropic three-dimensional behavior of a normally consolidated clay." *Can. Geotech. J.*, 30(5), 848–858.
- Li, C. (2005). "Mechanical response of fiber-reinforced soil." Ph.D. thesis, Univ. of Texas–Austin, Austin, TX.
- Li, X. S., and Dafalias, Y. F. (2002). "Constitutive modelling of inherently anisotropic sand behavior." *J. Geotech. Geoenviron. Eng.*, 128(10), 868–880.
- Liu, C.-N., Zornberg, J. G., Chen, T.-C., Ho, Y.-H., and Lin, B.-H. (2009). "Behavior of geogrid-sand interface in direct shear mode." *J. Geotech. Geoenviron. Eng.*, 135(12), 1863–1871.
- Liu, J., Wang, G., Kama, T., Zhang, F., Yang, J., and Shi, B. (2011). "Static liquefaction behavior of saturated fiber-reinforced sand in undrained ring-shear tests." *Geotext. Geomembr.*, 29(5), 462–471.
- Maher, M. H., and Gray, D. H. (1990). "Static response of sand reinforced with fibres." *J. Geotech. Eng.*, 116(11), 1661–1677.
- Michalowski, R. L. (1996). "Micromechanics-based failure model of granular/particulate medium with reinforcing fibers." *Technical Rep.*, Air Force Office of Scientific Research, Washington, DC.
- Michalowski, R. L. (2008). "Limit analysis with anisotropic fibre-reinforced soil." *Geotechnique*, 58(6), 489–501.
- Michalowski, R. L., and Čermák, J. (2002). "Strength anisotropy of fiber-reinforced sand." *Comput. Geotech.*, 29(4), 279–299.
- Michalowski, R. L., and Čermák, J. (2003). "Triaxial compression of sand reinforced with fibers." *J. Geotech. Geoenviron. Eng.*, 129(2), 125–136.
- Michalowski, R. L., and Zhao, A. (1996). "Failure of fiber-reinforced granular soils." *J. Geotech. Eng.*, 122(3), 226–234.
- Oda, M., Nemat-Nasser, S., and Konishi, J. (1985). "Stress-induced anisotropy in granular materials." *Soils Found.*, 25(3), 85–97.
- Palmeira, E. M., and Milligan, G. W. E. (1989). "Large scale direct shear tests on reinforced soil." *Soils Found.*, 29(1), 18–30.
- Park, S.-S. (2011). "Unconfined compressive strength and ductility of fiber-reinforced cemented sand." *Constr. Build. Mater.*, 25(2), 1134–1138.
- Ranjan, G., Vasan, R. M., and Charan, H. D. (1996). "Probabilistic analysis of randomly distributed fiber-reinforced soil." *J. Geotech. Engrg.*, 122(6), 419–426.
- Sadek, S., Najjar, S. S., and Freiha, F. (2010). "Shear strength of fiber-reinforced sands." *J. Geotech. Geoenviron. Eng.*, 136(3), 490–499.
- Santoni, R. L., and Webster, S. L. (2001). "Airfields and road construction using fiber stabilization of sands." *J. Transp. Eng.*, 127(2), 96–104.
- Sheng, D., Sloan, S. W., and Yu, H. S. (2000). "Aspects of finite element implementation of critical state models." *Comput. Mech.*, 26(2), 185–196.
- Shogaki, T., and Kumagai, N. (2008). "A slope stability analysis considering undrained strength anisotropy of natural clay deposits." *Soils Found.*, 48(6), 805–819.
- Silva Dos Santos, A. P., Consoli, N. C., and Baudet, B. A. (2010). "The mechanics of fibre-reinforced sand." *Geotechnique*, 61(10), 791–799.
- Sivakumar Babu, G. L., Vasudevan, A. K., and Haldar, S. (2008). "Numerical simulation of fiber-reinforced sand behaviour." *Geotext. Geomembr.*, 26(2), 181–188.
- Sonnenberg, R., Bransby, M. F., Hallett, P. D., Bengough, A. G., Mickovski, S. B., and Davies, M. C. R. (2010). "Centrifuge modelling of soil slopes reinforced with vegetation." *Can. Geotech. J.*, 47(12), 1415–1430.
- Tei, K., Taylor, R. N., and Milligan, G. W. E. (1998). "Centrifuge model tests of nailed soil slopes." *Soils Found.*, 38(2), 165–177.
- Uthayakumar, M., and Vaid, Y. P. (1998). "Static liquefaction of sands under multiaxial loading." *Can. Geotech. J.*, 35(2), 273–283.
- Wang, J., and Gutierrez, M. (2010). "Discrete element simulations of direct shear specimen scale effects." *Geotechnique*, 60(5), 395–409.
- Wei, W. B., and Cheng, Y. M. (2010). "Soil nailed slope by strength reduction and limit equilibrium methods." *Comput. Geotech.*, 37(5), 602–618.
- Wu, T. H., Mckinnel, W. P., III, and Swanston, D. N. (1979). "Strength of tree roots and landslides on Prince of Wales Island, Alaska." *Can. Geotech. J.*, 16(1), 19–33.
- Yao, Y. P., Lu, D. C., Zhou, A. N., and Zou, B. (2004). "Generalized nonlinear strength theory and transformed stress space." *Sci. China, Ser. E: Technol. Sci.*, 47(6), 691–709.
- Zdravković, L., Potts, D. M., and Hight, D. W. (2002). "The effect of strength anisotropy on the behaviour of embankments on soft ground." *Geotechnique*, 52(6), 447–457.
- Zornberg, J. G. (2002). "Discrete framework for equilibrium analysis of fibre-reinforced soil." *Geotechnique*, 52(8), 593–604.
- Zornberg, J. G., Cabral, A. R., and Viratjandr, C. (2004). "Behaviour of tire shred-sand mixtures." *Can. Geotech. J.*, 41(2), 227–241.